Mössbauer spectroscopy and chemical bonds in $BaFe_{12}O_{19}$ hexaferrite

2003 J. Phys.: Condens. Matter 15 5079

(http://iopscience.iop.org/0953-8984/15/29/319)

INSTITUTE OF PHYSICS PUBLISHING JOURNAL OF PHYSICS: CONDENSED MATTER

J. Phys.: Condens. Matter **15** (2003) 5079–5084 PII: S0953-8984(03)62386-6

Mössbauer spectroscopy and chemical bonds in $BaFe_{12}O_{19}$ hexaferrite

Fa-ming Gao[1], Dong-chun Li[1] and Si-yuan Zhang[2]

[1] Department of Materials Science and Chemical Engineering, Yanshan University, Qinhuangdao 066004, People's Republic of China
[2] Laboratory of Rare Earth Chemistry and Physics, Changchun Institute of Applied Chemistry, The Chinese Academy Sciences, Changchun 130022, People's Republic of China

E-mail: fmgao@ysu.edu.cn

Received 17 April 2003
Published 11 July 2003
Online at stacks.iop.org/JPhysCM/15/5079

Abstract

Barium hexaferrite was synthesized by chemical co-precipitation. Its Mössbauer spectra were obtained. A semi-empirical model, based on the Phillips theory of bonding, has been developed for quantitative explanation of the Mössbauer isomer shifts of Fe ions in $BaFe_{12}O_{19}$ crystals. The results show that, using the relationship between isomer shifts and covalency, the site assignments in hexaferrites will be resolved easily. This paper provides a powerful tool for studying other members of the hexagonal ferrimagnetic oxides family.

1. Introduction

The application of $BaFe_{12}O_{19}$, both pure and doped, has been of interest for some years due to its low production cost while providing excellent magnetic properties [1–3]. In particular, $BaFe_{12}O_{19}$ powders are currently being investigated for use in perpendicular recording [4]. $BaFe_{12}O_{19}$ is just one member of the family of hexagonal ferrimagnetic oxides [5], which can be described by the superposition of some fundamental structural blocks formed by a close packing of hexagonal or cubic-stacked layers with composition BaO_3 and O_4. In this framework, the metallic ions are located in octahedral and tetrahedral interstices. In the hexagonal M structure of $BaFe_{12}O_{19}$ [6], the Fe^{3+} ions occupy five different crystallographic sites. Three of the Fe^{3+} sites are octahedral (12k, $4f_2$, 2a), one is tetrahedral ($4f_1$), and one is trigonal bi-pyramidal (2b). Mössbauer spectroscopy has been used frequently to study this compound [7–11]. However, the Mössbauer spectra for these compounds showed complex structures that result from the overlap of Zeeman splitting patterns of the iron nuclei occupying different crystallographic positions in the lattice. Because of the superposition of sub-spectroscopies corresponding to different inequivalent Fe sites, site assignments in these ferrites have been proved to be a difficult task. It is well known, within each oxidation state, that the ranges of isomer shift

reflect the sum of covalency and bonding effects. Therefore, it is reasonable to investigate the isomer shift by starting from the chemical bond viewpoint.

2. Experiment

Barium ferrite was prepared by using the chemical co-precipitation method [9, 10]. All reagents were analytical grade. A solution of $Fe(NO_3)\cdot 9H_2O$, and $BaCl_2\cdot 2H_2O$ in water was poured into an $NaOH/Na_2CO_3$ alkaline solution. Thermal treatment of the co-precipitates that were obtained was performed at 1260 °C, respectively to each set of samples over 2 h. X-ray diffraction investigation is performed using Cu Kα radiation ($\lambda = 0.154\,06$ nm) in reflection mode. The result shows that the sample has single-phase Ba–M structure. Mössbauer experiments were carried out using a ^{57}Co/Pd source and a constant-acceleration spectrometer to collect the transmission spectra at room temperature. The spectrometer is calibrated using a standard α-Fe foil.

3. Theory

The dielectric description of covalency developed by Phillips and van Vecten [12] has been employed successfully in various fields. This theory provides us with a simple and clear scale for chemical bond covalency in crystals. In subsequent years, other workers [13–16] generalized the theory to the complex structure compounds.

Zhang [15] has pointed out that the properties of a crystal can be described by chemical bond parameters, and any complex crystal can be decomposed into different kinds of binary crystals. These binary crystals are related to each other and every binary crystal includes only one type of chemical bond. However, the properties of these binary crystals are different from those of real binary crystals, although their chemical bond parameters can be calculated in a similar way. In the theory, 'crystal formula' is a combination of sub-formula of chemical bonds. The sub-formula of any kind of chemical bond A–B in the multi-bond crystal $A_aB_b\ldots$ can be expressed by the following formula:

$$\left[\frac{N(\mathrm{B}-\mathrm{A})a}{N_{\mathrm{CA}}}\right]\mathrm{A}\left[\frac{N(\mathrm{A}-\mathrm{B})b}{N_{\mathrm{CB}}}\right]\mathrm{B}$$

where A, B, ... represent different elements or different sites of the same element in the crystal formula, and $a, b, \ldots$ represent the numbers of the corresponding element, $N(\mathrm{B}-\mathrm{A})$ represents the number of B ions in the coordination group of A ions, and N_{CA} represents the nearest coordination number of A ions. After decomposing the complex crystal into different kinds of binary crystals that form an isotropic system, and introducing an effective charge of valence electrons using the Pauling bond valence method, Levine's theory [13] can be used directly to calculated the chemical bond parameters in complex crystal compounds.

The macroscopic linear susceptibility χ can be resolved into contributions χ^μ from the various types of bonds or from the various binary crystals

$$\chi = \varepsilon - 1 = \sum_\mu F^\mu \chi^\mu = \sum_\mu N_{\mathrm{b}}^\mu \chi_{\mathrm{b}}^\mu \tag{1}$$

where ε is the dielectric constant, χ^μ is the total macroscopic susceptibility of a binary crystal composed of only one type of μ bond, F^μ is the fraction of the binary crystal composing the actual complex crystal, χ_{b}^μ is the susceptibility of a single bond of type μ in the corresponding binary crystal, and N_{b}^μ is the number of bonds per cubic centimetre:

$$\chi^\mu = (4\pi)^{-1}[(\hbar\Omega_{\mathrm{p}}^\mu)^2/(E_{\mathrm{g}}^\mu)^2] \tag{2}$$

where E_g^μ is the average energy gap for the type μ bond and Ω_p^μ is the plasma frequency obtained from the numbers of valence electrons of type μ per cubic centimetre, N_e^μ, using

$$(h\Omega_p^\mu)^2 = (4\pi N_e^\mu e^2/m). \tag{3}$$

N_e^μ is expressed as follows:

$$N_e^\mu = (n_e^\mu)^*/v_b^\mu \tag{4}$$

$$(n_e^\mu)^* = [(Z_A^\mu)^*/N_{CA}^\mu + (Z_B^\mu)^*/N_{CB}^\mu] \tag{5}$$

$$(k_F^\mu)^3 = 3\pi^2 N_e^\mu \tag{6}$$

where $(n_e^\mu)^*$ is the number of effective valence electrons per μ bond, k_F^μ is the Fermi wavenumber of valence electrons in a binary crystal composed of only one type of bond μ, and v_b^μ is the bond volume

$$v_b^\mu = (d^\mu)^3 \Big/ \sum_\nu [(d^\nu)^3 N_b^\nu] \tag{7}$$

where d^μ is the bond length. The average energy gap, E_g^μ, for every μ bond can be separated into homopolar E_h^μ and heteropolar C^μ parts:

$$(E_g^\mu)^2 = (E_h^\mu)^2 + (C^\mu)^2. \tag{8}$$

The ionicity and covalency of any type of chemical bond is defined as follows:

$$\begin{aligned} f_i^\mu &= (C^\mu)^2/(E_g^\mu)^2 \\ f_c^\mu &= (E_h^\mu)^2/(E_g^\mu)^2 \end{aligned} \tag{9}$$

where

$$E_h^\mu = 39.74/(d^\mu)^{2.48}\ (\text{eV}). \tag{10}$$

For any binary crystal AB_n-type compounds the heteropolar C^μ part is defined as

$$C^\mu = 14.4 b^\mu [(Z_A^\mu)^* + \Delta Z_A^\mu - n(Z_B^\mu)^*] e^{-k_s^\mu r_0^\mu}/r_0^\mu\ (\text{eV}) \tag{11}$$

$$\begin{aligned} r_0^\mu &= d^\mu/2 \\ k_s^\mu &= (4k_F^\mu/\pi a_B)^{1/2} \end{aligned} \tag{12}$$

where k_s^μ is the Thomas–Fermi screening wavenumber of valence electrons in a binary crystal composed of only one type of bond μ, a_B is the Bohr radius, and n is the ratio of element B to element A in the sub-formula. ΔZ_A^μ are correction factors from d-electron effects such as the crystal field stable energy and Jahn–Teller effect, etc [16, 17]. b^μ is proportional to the square of the average coordination number N_c^μ:

$$\begin{aligned} b^\mu &= \beta(N_c^\mu)^2 \\ N_c^\mu &= N_{CA}^\mu/(1+n) + nN_{CB}^\mu/(1+n) \end{aligned} \tag{13}$$

where b^μ depends on a given crystal structure. If the dielectric constant of the crystal is known, then the value of β can be deduced from the above equations. The bond parameters of the crystal, of which the dielectric constant is unknown, may also be estimated by using the β value of its isostructrual crystals.

We introduce the chemical environmental factor, h_e, which is expressed as [16]

$$h_e = \left(\sum \alpha_L^\nu f_c^\nu\right)^{1/2} \tag{14}$$

where α_L^ν is the polarizability of the ligand bond volume in the νth bond. The sum over ν runs over all the different types of the ligand bonds. For the μth bond, the polarizable coefficient α_0^μ can be obtained from the Lorentz–Lorenz equation

$$(\varepsilon^\mu - 1)/(\varepsilon^\mu + 2) = (4\pi/3)\alpha_0^\mu. \tag{15}$$

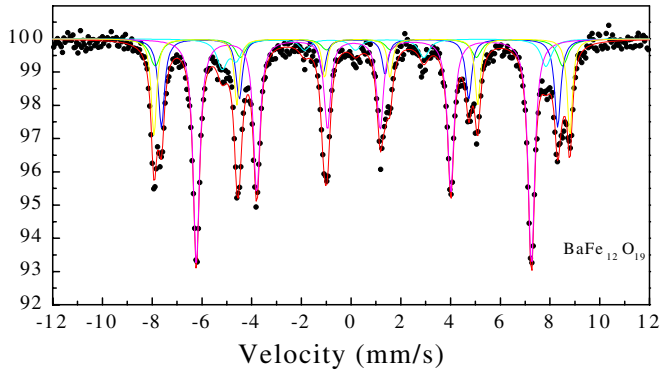

Figure 1. Mössbauer spectra of the precipitate method sample of Ba *M*.
(This figure is in colour only in the electronic version)

The polarizabilities of the bond volume is

$$\alpha_{\mathrm{b}}^{\mu} = \alpha_0^{\mu} v_{\mathrm{b}}^{\mu}. \tag{16}$$

The polarizabilities of the ion volume in the μth bond are

$$\alpha_{\mathrm{A}}^{\mu} = [(r_{\mathrm{A}}^{\mu})^3/[(r_{\mathrm{A}}^{\mu})^3 + (r_{\mathrm{B}}^{\mu})^3]]\alpha_0^{\mu} \tag{17}$$

$$\alpha_{\mathrm{B}}^{\mu} = [(r_{\mathrm{B}}^{\mu})^3/[(r_{\mathrm{A}}^{\mu})^3 + (r_{\mathrm{B}}^{\mu})^3]]\alpha_0^{\mu} \tag{18}$$

where r_{A}^{μ} and r_{B}^{μ} are radii of the A and B atoms in the μth bond, respectively.

The significant aspect of Mössbauer spectroscopy is the discovery of the isomer shift. It has been known that the ^{57}Fe isomer shift can provide extensive and valuable information about the local chemical environment of iron. For a given oxidation state, a correlation between the isomer shift δ and the chemical environmental factor h_{e} is found [16]. This can be written as:

$$\delta(^{57}\mathrm{Fe}) = \delta_0 + bh_{\mathrm{e}} \ (\mathrm{mm\ s^{-1}},\ \text{relative to } \alpha\text{-Fe at room temperature}) \tag{19}$$

where, for isolated ions Fe^{m+} and $b = -0.7$, it contains nuclear parameters. When h_{e} is equal to zero, then $\delta = \delta_0$, which is the isomer shift of the free-ion state. For an isolated high-spin $\mathrm{Fe}^{2+}(\mathrm{d}^6)$ and $\mathrm{Fe}^{3+}(\mathrm{d}^5)$, δ_0 is 1.68 and 0.87 mm s^{-1}, respectively.

4. Results and discussion

Mössbauer spectroscopy of the sample synthesized by chemical co-precipitation shows the typical pattern of five sextuplets due to iron's 2a, 4f$_1$, 12k, 4f$_2$, and 2b ions (see figure 1).

For $BaFe_{12}O_{19}$, according to theory [15], the crystal formula of $BaFe_{12}O_{19}$ can be converted into the sub-formula equation below:

$$\begin{aligned}
BaFe_{12}O_{19} &= BaFe(1)Fe(2)Fe(3)_2Fe(4)_2Fe(5)_6O(1)_2O(2)_2O(3)_3O(4)_6O(5)_6 \\
&= \tfrac{1}{2}BaO(3)_{12/5} + \tfrac{1}{2}BaO(5)_3 + Fe(1)O(4)_{3/2} + \tfrac{2}{5}Fe(2)O(1)_{5/4} \\
&\quad + \tfrac{3}{5}Fe(2)O(3) + \tfrac{1}{2}Fe(3)O(2) + \tfrac{3}{2}Fe(3)O(4) + Fe(4)O(3)_{6/5} \\
&\quad + Fe(4)O(5)_{3/2} + Fe(5)O(1)_{3/2} + 2Fe(5)O(2)_{3/2} + 2Fe(5)O(4)_{3/2} \\
&\quad + Fe(5)O(5)_{3/2}.
\end{aligned}$$

Using the β value (0.097) of the isostructrual crystal $LaMgAl_{11}O_{19}$ [18], the chemical bond parameters of each type of chemical bond are calculated and listed in table 1. The chemical

Table 1. The chemical bond parameters of $BaFe_{12}O_{19}$.

Bond type	Cation site	Anion site	$N_e^m u$	k_F^μ	E_h^μ	C^μ	f_c^μ	χ^μ	α_L^v
BaO(3)	2d	6h	0.063	1.231	2.717	14.899	0.033	0.157	
BaO(5)	2d	$12k_2$	0.068	1.263	2.914	11.519	0.060	0.468	
Fe(1)O(4)	2a	$12k_1$	0.604	2.615	7.123	13.504	0.218	3.378	0.393
Fe(2)O(1)	2b	4e	0.797	2.868	5.048	11.037	0.173	7.429	0.822
Fe(2)O(3)	2b	6h	0.502	2.459	8.539	11.306	0.363	3.235	0.301
Fe(3)O(2)	$4f_1$	4f	0.712	2.762	8.153	7.415	0.547	8.062	0.473
Fe(3)O(4)	$4f_1$	$12k_1$	1.186	3.275	8.153	10.381	0.382	9.500	0.489
Fe(4)O(3)	$4f_2$	6h	0.724	2.778	6.517	19.551	0.100	2.156	0.336
Fe(4)O(5)	$4f_2$	$12k_2$	0.422	2.320	7.404	10.124	0.349	3.474	0.361
Fe(5)O(1)	12k	4e	0.412	2.302	7.257	9.924	0.349	3.532	0.375
Fe(5)O(2)	12k	4f	0.528	2.500	6.371	12.052	0.218	3.717	0.459
Fe(5)O(4)	12k	$12k_1$	0.341	2.161	6.208	9.417	0.303	3.451	0.460
Fe(5)O(5)	12k	$12k_2$	1.006	3.100	7.761	18.216	0.154	3.385	0.335

Table 2. Mössbauer isomer shifts [11] of $BaFe_{12}O_{19}$ (mm s^{-1}).

Ion	Fe(1)	Fe(2)	Fe(3)	Fe(4)	Fe(5)
Site	2a	2b	$4f_1$	$4f_2$	12k
h_e	0.716	0.783	0.905	0.691	0.783
δ_{calc}	0.37	0.32	0.24	0.39	0.32
δ_{exp} [11]	0.38	0.32	0.24	0.39	0.35
δ_{exp} (this work)	0.34	0.32	0.26	0.39	0.35

Table 3. Iron sublattices in the crystalline structure of $BaFe_{12}O_{19}$ hexagonal ferrite.

Sublattice	Coordination	No of iron ions per formula unit	δ (mm s^{-1})	Average bond length	N_e^μ (average values)	f_c^μ (average values)
$4f_2$	Octahedral	2	0.39	2.021	0.573	0.225
2a	Octahedral	1	0.38	2.000	0.604	0.218
12k	Octahedral	6	0.35	2.028	0.606	0.247
2b	Bi-pyramidal	1	0.32	2.035	0.620	0.287
$4f_1$	Tetrahedral	2	0.24	1.894	1.068	0.424

environmental factor for Fe sites in Ba–*M* crystals is obtained using equation (14) and the isomer shifts of Fe^{n+} were calculated from equation 19. The results are shown in table 2. From table 2, it is clearly seen that the calculated results of Mössbauer isomer shifts in various crystallographic positions are in good agreement with their experimental values. This also shows that the chemical bond parameters calculated by us are reasonable.

In order to classify the most obvious trends in isomer shift, the room-temperature values of isomer shift and some parameters describing their local environments have been listed in table 3. It is generally admitted that, for a given oxidation state and for identical ligands, a decrease in the iron coordination number leads to a decrease in the isomer shift. One mechanism has been proposed to explain this result: an increase in the covalency of the iron–ligand bonds [19]. As shown in table 3, our calculated covalency of various Fe^{3+} sites could support the above point of view.

For the observed decrease in the isomer shifts with increasing N_e^{μ} in table 3, an explanation should be sought in the physical nature of this hyperfine interaction. For a given source matrix, the isomer shift is a measure for the electron density at the absorbing nuclei and is proportional to $|\Psi(0)|^2$. Neglecting relativistic effects, only s-electrons possess a non-zero probability of entering the nuclear volume and therefore the isomer shift is a good approximation proportional to the s-electron density at the nucleus, $|\Psi_s(0)|^2$. Since the nuclear radius of ^{57}Fe in the first excited state is smaller than that in the ground state, an increasing δ implies a decreasing s-electron density at the absorbing nuclei. In $BaFe_{12}O_{19}$ hexagonal ferrite, a decreasing N_e^{μ} of iron sites could represent decreasing s-electron density and result in an increase in the isomer shifts.

It might be tempting to assume that an increase in the Fe–O distances should induce a decrease in the overlap between the 4s orbital of iron and the ligand orbital, and therefore lead to an increase in the isomer shift. However, we have to admit that such a correlation is by no means obvious in table 3—for example, ($Fe^{3+}O_5$) triangular bipyramidal coordination possesses larger length than ($Fe^{3+}O_6$) octahedral coordination, but the corresponding average isomer shift is definitely smaller in ($Fe^{3+}O_5$). So, the correlation between the isomer shift and the length of the iron–ligand bonds appears to be groundless.

In addition, the general belief is that the strong anisotropy of the hexagonal compound $BaFe_{12}O_{19}$ is, to a great extent, due to one of the Fe ions in a bi-pyramidal site. The calculated results of the susceptibility that we have reported here can support the above view. From table 2, our calculated results show that the susceptibility χ^{μ} (Fe_2O_1, parallel to the c-axis) $\gg \chi^{\mu}$ (Fe_2O_3, perpendicular to the c-axis).

5. Conclusion

In conclusion, starting from the chemical bond viewpoint, we investigated all constituent chemical bonds in $BaFe_{12}O_{19}$. Since the chemical isomer shift behaves independently of the other two hyperfine interactions, and is conveniently considered first, by using the relationship between isomer shifts and covalency the site assignments in hexaferrites can be resolved easily. This paper provides us with a powerful tool for studying other members of the family of hexagonal ferrimagnetic oxides.

References

[1] Gomi M, Cho J and Abe M 1997 *J. Appl. Phys.* **82** 5126
[2] Harris J E, Harrell J W, Parker F T and Kitahata S 1997 *J. Appl. Phys.* **81** 3824
[3] Garcia D, Muro M, Batlle X, Labarta A, Gonzalez J M and Montero M I 1997 *J. Appl. Phys.* **81** 3812
[4] Morisako A, Matsumoto M and Naoe M 1996 *J. Appl. Phys.* **79** 4881
[5] Braun P J 1957 *Philips Res. Rep.* **12** 491
[6] Obradors X, Collomb A, Pernet M, Samaras D and Joubert J C 1985 *J. Solid State Chem.* **56** 171
[7] Oh Y J, Shim I B, Park H J, Park S I, Lee Y J, Lee S W and Kim C S 1994 *J. Appl. Phys.* **76** 6877
[8] Clark T M, Evans B J, Thompson G K and Freeman S 1999 *J. Appl. Phys.* **85** 5229
[9] Jacobo S E, Domingo-pascual C, Rodriguez-clemente R and Blest M A 1997 *J. Mater. Sci.* **32** 1025
[10] Matutes-Aquino J, Diaz-Castanon S, Mirabal-Garcia M and Palomares-Sanchez S A 2000 *Scr. Mater.* **42** 295
[11] Belozerskii G N and Khimich Yu P 1975 *Fiz. Tverd. Tela* **17** 1352
[12] Phillips J C 1970 *Rev. Mod. Phys.* **42** 317
[13] Levine B F 1973 *J. Chem. Phys.* **59** 1463
[14] Meng Q B, Wu Z J and Zhang S Y 1998 *J. Phys. Chem. Solids* **59** 633
[15] Zhang S Y 1991 *Chin. J. Chem. Phys.* **4** 109
[16] Gao F M, Li D C, He J L, Yu D L, Tian Y J and Zhang S Y 2002 *Physica* C **371** 151
[17] Gao F M and Zhan S Y 2000 *Chin. J. Inorg. Chem.* **16** 751
[18] Gao F M and Zhan S Y 2001 *J. Synth. Cryst.* **30** 198
[19] Menil F 1985 *J. Phys. Chem. Solids* **46** 763